

Analytical description of memory loss based on neuronal synaptic strength

Hillel Sanhedrai^{1*}, Shlomo Havlin¹ & Hila Dvir^{1*}

December 15, 2022

1. *Department of Physics, Bar-Ilan University, Ramat-Gan, Israel*

* **Correspondence:** *hillel.sanhedrai@gmail.com (HS), dvirhila@gmail.com (HD)*

Long-term-memory (LTM) and short-term-memory (STM) are both described as a decaying function with time. However, this decaying memory function is currently obtained empirically, by direct tests of subjects, and its physiological meaning have not yet been fully understood. Here we provide an analytical description of memory loss based on the averaged synaptic strength, ω , which is a physiological parameter that is believed to be associated with memory. This analysis sheds light on unknown aspects of the memory mechanism, and particularly for the less known intermediate-term-memory (ITM), of time scale between LTM and STM. Our analytical description suggests answers to important questions related to memory: why do LTM and STM have correlated performances? why do electrophysiological experimental protocols, imitating LTM, last only up to weeks while regular LTM lasts decades? and what is the mechanism for ITM? Our results may have clinical implications for medical treatments of patients with memory impairments.

The first experimental studies of human memory have been performed by Hermann Ebbinghaus, who was also the first to describe, in 1885, the memory as a function that decays with time, termed “forgetting curve”- marking the memory retention decline in time [1]. Ebbinghaus has also approximated this decline using a logarithmic function [1]. Nowadays, the memory decay is quantified usually as an exponential decay with two time constants: fast and slow (with a factor of ~ 10 between them) [2, 3]. However, the current quantitative descriptions of memory loss are mainly empirical expressions, based on human tests, and are not based on any underlying physiological mechanism. Here we suggest an analytical description of memory loss using a well known physiological state parameter - averaged synaptic strength ω . Specifically we show that the value of ω can describe the time constant loss for all memory types: long-term memory (LTM), short-term memory (STM) and intermediate-term memory (ITM). Based on this, we also provide mechanistic understanding for the intermediate behavior, ITM [4], a less defined phenomenon on the spectrum between STM and LTM.

Since memory is regarded as a process where knowledge is retained, biophysical models have been using persistent activity of the synaptic current to describe memory in the spiking-neuron level [5]. However, electrophysiological studies suggest that memory cannot be comprehended only from the spiking activity, but rather is based also on facilitation of the synaptic networks connections [6]. It is accepted that memory formation depends on changes in synaptic efficiency, by strengthening the connections between neurons [7]. Hebb [8] proposed that when two neurons are activated simultaneously, the appropriate synapse will be strengthened accordingly. However, there is currently no analytical theory that relates the memory loss curve directly to synaptic strength, which is our goal here.

At present, the working memory models, which are based on neurons activity in a network, usually use persistent activity through recurrent excitation, analyzing the memory using phase diagram in the [current] vs. [afferent stimulating current] space [9, 5, 10]. Alternatively, other models analyze memory using phase diagram in the [averaged firing rate] vs. [synaptic strengths] space [11, 12]. Here we based our analysis on the [current] vs. [synaptic strengths] space, for which we perform infinitesimal analysis near critical values. This approach yields an analytical expression for the memory time constant as a function of synaptic strength, and furthermore lead us to develop a theory regarding the mechanism of ITM.

As a base for our ITM memory data analysis, we use results of electrophysiological experiments of young and old rats, measured by excitatory postsynaptic potentials (EPSP) [7]. The common belief is that those experiments are the physiological basis of memory which accompanies plasticity in synaptic connections [7]. However, it is not known yet what is their relationship to LTM, as those experiments persist only up to weeks. Our analysis of EPSP data suggests that in those cases the memory will decay to forgetfulness similar to ITM while indicating the mechanism for this behavior as follows. We suggest that ITM starts close to criticality as either STM (ITM-STM-driven) or LTM (ITM-LTM-driven). For example, we show that aged rats have weaker ω synaptic connections, and hence tend to have ITM according to the ITM-STM-driven scenario, while young rats have stronger synaptic connections and therefore tend to show the ITM-LTM-driven scenario. Our results also suggest that both scenarios are different in their nature: deterministic for the ITM-STM-driven and stochastic for the ITM-LTM-driven.

Whether there exists a clear distinction between the LTM and STM, is a highly controversial subject [13]. To clarify this, we provide here evidence indicating that the memory is indeed a spectrum containing both characteristics, but there is also a genuine distinction between LTM and STM. Our approach, based on analysis of synaptic strength, enables the description of the temporal dynamic of STM, LTM and ITM, and specifically elucidate the yet unknown aspects of forgetfulness using deterministic as well as stochastic tools.

Results

Electrophysiological studies suggest that the main mechanism of memory formation is imprinted in the alterations of neurons network synaptic efficiency [6–8]. We thus analyze the memory in the ω -space (the average weight, see Eq. (4) and Fig. 1) instead of the conventional phase diagram analyzed in current/voltage-space. Moreover, as memory formation is obtained when a persistent electrical activity is present long after the afferent current is lost [5, 7], i.e., when $I_{\text{Aff}} = 0$ (see Eq. (5)), it further motivate us to analyze the memory in the ω -space instead of the common I_{Aff} -space. Specifically, we are interested in the dynamic of the memory formation in proximity to stimulating current I_{Aff} , as well as long after I_{Aff} vanishes.

The basic model

A common model of working memory is based on sustained excitation activity of highly connected neuronal cells. This concept was introduced in the Hopfield model [14, 15], which describes the variables as the neuronal membrane potential [15] or current [9, 5]. The model was formalized as,

$$\tau \frac{dI_i}{dt} = -I_i + \sum_{j \neq i} w_{ij} \ln \left(\frac{I_j}{C} \right) \theta(I_j - C) + I_{\text{Aff}}, \quad (1)$$

where I_i represents the current in neuron i , τ is the time constant. Here, $\theta(x)$ is the Heaviside step function, determining an excitation threshold C , where only above C the current of neuron j impacts neuron i . I_{Aff} is the external current excitation, which could be obtained due to external stimulation (e.g., sensory stimulation). In Eq. (1), w_{ij} represent the interaction strengths (synaptic strength) between neurons i and j , constructed as a complete graph (all neurons are connected to each other).

Here we hypothesize that the weights w_{ij} vary with a value that is imprinted by the person's characteristics.

Moreover, we assume that w_{ij} depends also upon the strength of the external stimulation, specifically, we assume that high external input derives high neuronal connections w_{ij} . Therefore, our analysis here will be based on a memory phase diagram in the ω -space as in Fig. 1, where ω is the average over all weights w_{ij} .

This definition of ω , as the average weight, is analogous to the analysis of Eq. (1) using a Mean-Field (MF) approximation [16]. Specifically, in order to execute complex tasks such as memory, the brain neurons become highly connected [17–19], with a networking properties close to a complete graph, what makes the MF more accurate. This, in addition to applying $\frac{1}{N} \sum_{j=1}^N$ operator on Eq. (1), yields (see SI Section S.1):

$$\tau \frac{dI}{dt} = -I + \omega(N-1) \ln\left(\frac{I}{C}\right) \theta(I-C) + I_{\text{Aff}}, \quad (2)$$

where

$$I = \frac{1}{N} \sum_{j=1}^N I_j, \quad (3)$$

and with defining ω as

$$\omega = \frac{1}{N(N-1)} \sum_{j \neq i} w_{ij}. \quad (4)$$

Thus, I is the average current across the neurons, and ω is the average interaction weight between neurons.

Concerning memory, it is of importance to study the sustained current when $I_{\text{Aff}} = 0$,

$$\tau \frac{dI}{dt} = -I + \omega(N-1) \ln\left(\frac{I}{C}\right) \theta(I-C). \quad (5)$$

We next track the fixed points of Eq. (5) by setting $dI/dt = 0$, which yields three solutions for the average current I as a function of the average weight ω : two stable and one unstable solutions. The ω -space splits into two areas. Indeed, Fig. 1 (see also Fig. S1 in SI) shows exactly this: small values of ω yield a single dormant state (red), whereas large ω yields three fixed points (including two steady states, active (blue) and dormant (red)). We assume that the active state enables the existence of a long-range memory (LTM) for large enough ω , while for small ω the memory cannot stay for long, hence it is the region of a short-range memory (STM).

To find the critical (tipping) point (ω_c, I_c) of the transition from STM to LTM, we notice that this point is a junction of stable fixed point (continuous blue line in Fig. 1) and unstable one (dashed green line). This requirement yields (see SI Section S.3),

$$\omega_c = \frac{e \cdot C}{N-1}, \quad I_c = e \cdot C. \quad (6)$$

We conclude from this that $\omega > \omega_c$ is the condition for the creation of LTM, otherwise the memory is not preserved and the current decays to zero, hence $\omega < \omega_c$ is an STM region.

In the following analyses we explore the impact of interaction (synaptic) weights on fundamental temporal memory characters through theoretical and simulation results compared to experimental wet-lab properties. The experimental wet-lab relates to hippocampal of anesthetized young and aged rats model [7]. Note that using hippocampal model is a widely used paradigm of simple brainlike structures [20].

Long-term memory

In this Section we study the regime in ω -space of $\omega > \omega_c$, where LTM is observed, and analyze the memory dynamic when converging to a steady state. Specifically, we show that the current converges to its stable state exponentially with a typical time constant (representing the memory length) that depends on the average weight ω .

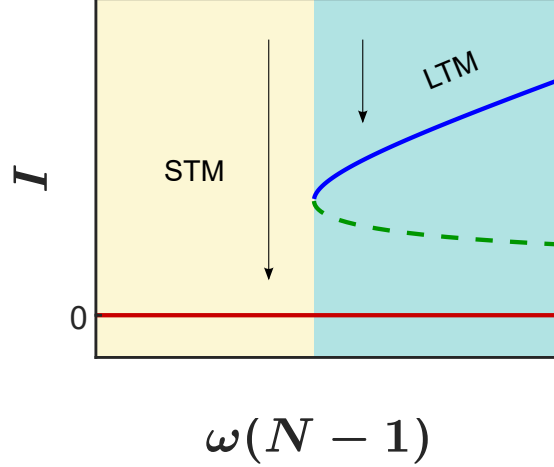


Figure 1: **Memory phase diagram.** The phase diagram in ω -space obtained from Eq. (5). The blue and the red continuous lines represent the steady states solutions, while the dashed green line represents an unstable state separating between the two basins of attraction. Note that according to Eq. (4), the value of $\omega(N-1)$ is actually the mean synaptic weight.

For a steady state LTM solution, the derivative of the current vanishes in Eq. (5) obtaining:

$$0 = -I_{LT} + \omega(N-1) \ln(I_{LT}/C), \quad (7)$$

where I_{LT} is the persistent current that yields the LTM (steady-state solution).

Here we are interested in describing the dynamics of LTM using Eq. (5) in two different limits: $I \gg I_{LT}$ and when I approaches I_{LT} (when $I \rightarrow I_{LT}$).

For the first limit ($I \gg I_{LT}$), the behavior is trivial: since I is very large it can be assumed that $I \gg \ln I$, so that Eq. (5) can be written approximately as $\tau dI/dt \sim -I$, and therefore an exponential decay with a typical time τ is obtained,

$$I(t) \sim \exp(-t/\tau). \quad (8)$$

In the second limit close to I_{LT} (when $I \rightarrow I_{LT}$), we expand Eq. (5) for $I = I_{LT} + \delta I$ where δI is small (see details in SI Section S.4), and obtain,

$$\tau \frac{d\delta I}{dt} \approx - \left(1 - \frac{1}{\ln(I_{LT}/C)} \right) \delta I.$$

This implies an exponential decay with the typical time decay,

$$\tau_{LT} = \frac{\tau}{1 - \frac{1}{\ln(I_{LT}/C)}}. \quad (9)$$

Note that this exponent is valid under the condition $\delta I/I_{LT} \ll \ln(I_{LT}/I_c)$ as aforementioned, namely within a region above the steady memory, see Fig. 2 a. The range of this valid region is getting small close to criticality.

Figure 2 b shows results from simulating Eq. (1) with $I_{Aff} = 0$ for the LTM case, that is for $\omega > \omega_c$, showing the average current, I , temporal decay. Each colored line relates to different value of $\Delta\omega$ normalized by ω_c . Particularly, for all values of $\Delta\omega/\omega_c$ two exponential decays can be observed. The first exponent, at short time scales (in the beginning of the simulations), is τ (the time scale), which appears for all $\Delta\omega/\omega_c$ values, in accordance to Eq. (8) (Fig. 2 b dashed orange line). The second exponent, at long time scales (towards the end of the simulation and close to steady state), a more moderate decay is obtained with an exponential value that fits well to the τ_{LT} as depicted in Eq. (9) (Fig. 2 b, four dashed lines). Note that the first exponent is smaller than the second exponent,

which also fits well Eq. (9) implying that $\tau_{LT} > \tau$.

Next, we evaluate τ_{LT} when ω is close to the critical value ω_c from above. To track the behavior in proximity of ω_c (for small $\Delta\omega$), we expand Eq. (7) using $\omega = \omega_c + \Delta\omega$ and $I_{LT} = I_c + \delta I_{LT}$ (see SI Section S.4.1). Recalling $I_c = e \cdot C$, and $\omega_c = e \cdot C / (N - 1)$ (Eq. (6)) we get

$$\delta I_{LT} \approx I_c \sqrt{2\Delta\omega/\omega_c}.$$

Substituting this into Eq. (9), we finally obtain,

$$\tau_{LT} \approx \frac{\tau}{\sqrt{2\Delta\omega/\omega_c}}. \quad (10)$$

This relation, Eq. (10), is in excellent agreement with our simulation results as illustrated in Fig. 2 c. Fig. 2 c summarizes the values of the exponential time decay, τ_{LT} , as obtained from the simulations of the current I close to its steady state (the gray area in Fig. 2 a and the straight lines close to steady-state in Fig. 2 b). It is clearly seen that the relation between $\Delta\omega/\omega_c$ and τ_{LT} is a power law with an exponent $-1/2$, supporting Eq. (10). Note, as expected, that for small values of $\Delta\omega/\omega_c$, i.e. when ω is close to ω_c (small $\Delta\omega$), the simulation results are more accurately described by a $-1/2$ slope.

After investigating the model theoretically and verifying it by simulations, we explore the theoretical parameter ω and its relation to actual electrophysiological experiments of measuring memory data EPSP. We used EPSP data measuring long-term potentiation (LTP) [7], which is a phenomenon observed in brain areas involved in memory storage such as the hippocampus, and it describes long lasting increase of the EPSP after stimulation. The common belief is that LTP is the physiological basis of memory which accompanies plasticity in synaptic connections [7]. Fig. 2 d shows the LTP dynamics as experimentally measures in young rats [7] (blue dots) compared to our theoretical model current dynamics as simulated for $(\omega - \omega_c)/\omega_c = \Delta\omega/\omega_c = 0.006$ (red line). The excellent agreement between the data and the model suggests indeed that the average weight ω relation to the critical weight ω_c is $\omega = 1.006 \cdot \omega_c$. Thus, in this data of anesthetized young rats, the average synaptic weight is fairly close to the critical LTM weight. Therefore, given enough time their memory will eventually decay to zero, as indeed occurs in this LTP memory data after a week [7], faster than the common LTM. Nevertheless, the proximity to criticality is not a sufficient condition in order for the system to move from just above critical point to forgetfulness. For that additional stochasticity is needed, which can arise from the synapses stochastic nature, as we discuss in details below in Section ‘Intermediate-term memory(ITM): LTM-driven’.

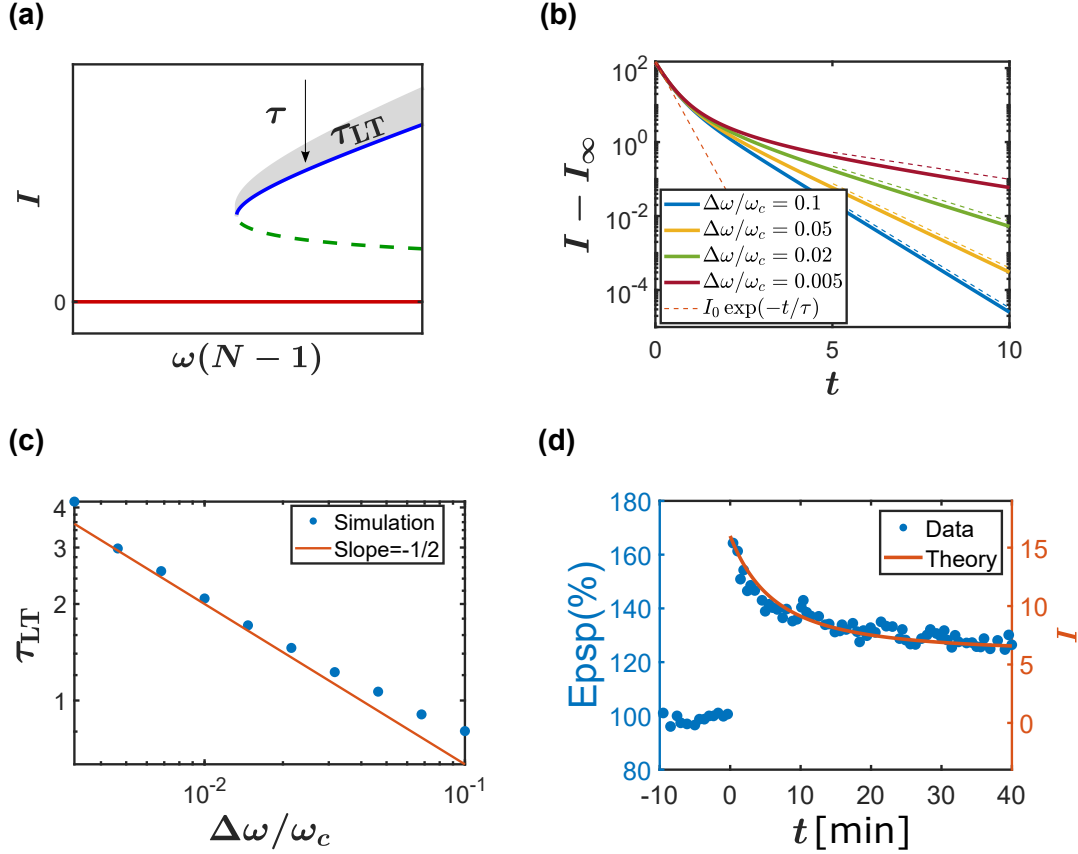


Figure 2: Long-term memory temporal decay. (a) The current converges to a positive steady state because the average synaptic weight ω is above criticality $\omega > \omega_c$ and the system is in the active region. However, we identify two different typical time constants, long and short, for the decay of the memory. Far from the steady state there is a universal time decay τ while close to the final state (gray area) there is a larger varying time decay τ_{LT} . (b) The decay of the average current I with time is exponential with fast (at the beginning) and slow (towards the end) exponential decay. The fast and slow exponents show characteristic time constants τ and τ_{LT} , respectively fit well to their theoretical descriptions in Eq. (8) and Eq. (9), which are marked in dashed lines. (c) Here we provide a support for the analytical approximation, Eq. (10), for small $\Delta\omega$. Simulations in panels (b) and (c) were obtained for a network of size $N = 100$ neurons, threshold of $C = 2$, $\tau = 0.25$ and initial condition (by stimulating current $I_{A\#}$) of $I_0 = 150$. (d) Memory experimental data as collected from anesthetized young rats model [7] (blue) compared to our model (red) with $C = 2$, $\tau = 3$, $I_0 = 16$ and $\Delta\omega/\omega_c = 0.006$ (i.e., $\omega = 1.006 \cdot \omega_c$) yielding $\tau_{LT} \approx 27$ min. Note that the value of $\omega/\omega_c = 1.006$ is normalized, and therefore is not affected by units or scaling parameters which affect both τ and τ_{LT} (see Eq. (10)). Hence, while other parameters sets might yield same current temporal configuration, the value of ω/ω_c is resilience and fixed per configuration.

Short-term memory (STM)

In the previous Section we proposed a theoretical framework for understanding the LTM dynamics, in this Section we provide an analytical description for the STM. We assume that for the STM case, the system resides in the region which includes only the dormant steady state, and that in the ω -phase it presents average synaptic weight of $\omega < \omega_c$. Similar to the analysis for LTM, for STM we also explore the time decay of the current dynamics, but towards zero (compared to the decay towards I_{LT} for the LTM).

To explore Eq. (5) for STM, i.e. for $\omega < \omega_c$, we analyze the current around its critical value I_c (which is described in Eq. (6)). We focus our analysis on this regime for the following reasons. (i) We are interested in the behavior changes when approaching criticality, (ω_c, I_c) . (ii) As we show next, we find that the region close to I_c yields an exponential decay towards zero which is similar to empirical results [21].

To this end, we analyze the evolution of $I(t)$ around I_c . Since here we explore STM, we hypothesize that $\omega < \omega_c$ and therefore, $\omega = \omega_c - \Delta\omega$ (this is opposed to the LTM where $\omega > \omega_c$ which defines $\omega = \omega_c + \Delta\omega$). Expanding Eq. (5) at $I = I_c + \delta I$, for small deviation δI (see SI Section S.5), we obtain,

$$\tau \frac{dI}{dt} \approx -\frac{\Delta\omega}{\omega_c} I, \quad (11)$$

where we neglect the second order term, i.e. assuming $(\delta I/I_c)^2 \ll \Delta\omega/\omega$. Thus, this region gets smaller close to criticality, as illustrated in Fig. 3 a (region marked in gray).

Finally, Eq. (11) yields

$$I(t) \sim \exp(-t/\tau_{ST}), \quad (12)$$

where the time decay is

$$\tau_{ST} = \frac{\tau}{\Delta\omega/\omega_c}. \quad (13)$$

Equation (13) suggests that the time decay τ_{ST} becomes larger when approaching ω_c , where at ω_c the decay is not anymore exponential but becomes a power-law (by applying $\Delta\omega = 0$ and considering also second order terms in the expansion), i.e., a very slow decay of memory. For ω which are far below ω_c , the time decay gets smaller, even smaller than τ . Physiologically, this is reasonable, as for a small memory stimulation, a smaller average synaptic weight ω is formed (i.e., far from critical ω_c), which in turn obtains a shorter time decay τ_{ST} and the memory is very brief.

Figure 3 b shows τ_{ST} , the time decay of the current I , for $\omega < \omega_c$, for four different values of $\Delta\omega/\omega_c$. It can be seen that indeed, when ω is farther from ω_c (for high $\Delta\omega$), the current decays faster, e.g., the red line vs. the blue line. Moreover, this decay appears to be straight in the semi-logarithmic plot around I_c (the value of I_c is marked in horizontal black line), i.e., the current I exponentially decays to zero. The dashed lines mark the slopes obtained from Eq. (13), showing an excellent agreement with I at the region where $(\delta I/I_c)$ is small (marked in gray). Fig. 3 c summarizes the fit of τ_{ST} between the theory, Eq. (13) (red line), and the simulations (blue dots), showing an excellent agreement.

While the above analysis is based on theory and simulations, we ask next: which STM empirical test can reflect the dependency of τ_{ST} on $\Delta\omega/\omega_c$ similarly to Fig. 3 b? One such possibility is when ω changes while ω_c remains constant, thus monotonous change in $(\omega - \omega_c)/\omega_c = \Delta\omega/\omega_c$ can be obtained. We suggest that this scenario is related to STM tests performed on the same participant (same ω_c) but with different word presenting rate. Indeed, Fig. 3 d shows STM test results as obtained from a typical participant recall performances dynamic across time [21]. Since Fig. 3 d results relates to the same participant tested with same number of lists items we assume that ω_c remains constant, and since only the word presenting rates are different we assume that only $\Delta\omega$ varies (reflecting changes in the average synaptic weights, ω). This assumption is supported by a qualitative comparison between Fig. 3 d to Fig. 3 b, though further study is required to support this finding.

In summary, looking at the time durations of LTM, τ_{LT} , (Eq. (10)) vs. STM τ_{ST} (Eq. (13)), we find that both equations depend on τ and ω_c (though having different relations). This observation can provide the theoretical explanation for behavioral tests that found correlation between STM and LTM [22, 23]. Namely, subjects with strong STM tend to have strong LTM, which could be explained by our model suggesting that the dynamics of both STM and LTM depend on same variables: τ and ω_c .

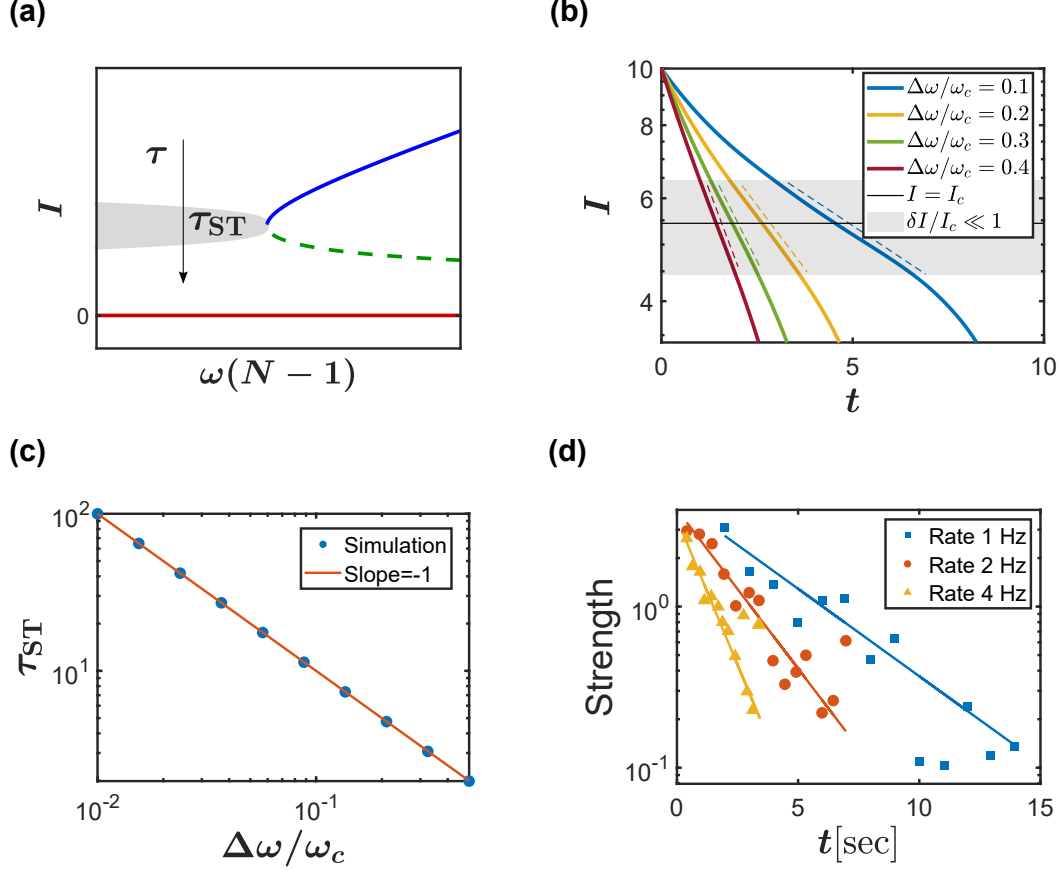


Figure 3: Short-term memory temporal decay. (a) The current decays to zero because the weight is below criticality, $\omega < \omega_c$, thus the system is in the dormant region. The regime where τ_{ST} is relevant is marked in gray. (b) Simulation results with four different $\Delta\omega/\omega_c$ values marked in colored lines. The gray area around I_c marks the range where the decay of I in time is exponential with typical time $\tau_{ST} = \tau/(\Delta\omega/\omega_c)$ (dashed lines), which is in good agreement with theory, Eq. (13). Note that we show I only up to the threshold value C since below it there exists no relevant signal. (c) It is seen that τ_{ST} from the simulated curves (like in (b)) scales as $\Delta\omega^{-1}$, which supports the theory, Eq. (13). The simulations results in panels (b)-(c) were obtained based on a network of $N = 100$ neurons, $C = 2$ and $\tau = 1$ min. (d) Recalling of a limited list is a common procedure to quantify STM empirically. The ability to recall words/numbers from a list depends also on the test itself. Here we show an example from empirical tests [21] for several word presenting rates. Comparing this panel to panel (b) shows how STM dynamics across different rates can be modeled by using different synaptic connection strengths. The lines are the analytical theory fittings of the empirical data with time decays $\tau = 4, 2.2, 1.2$ min. Note that towards 10sec, the blue dots (rate of 1Hz) markedly reach below the exponential fitting blue line, which has some resemblance to the curved lines in panel (b) when I reaches below the valid gray area (mostly noted in the blue symbols in panel (b)).

Intermediate-term memory (ITM): STM-driven

In this Section and the following ones we focus in the ITM. ITM, which has been recently introduced, has characteristic time duration between LTM to STM, however, it disappears entirely before LTM is maintained [4]. Here we suggest two possible scenarios as mechanisms for ITM, both scenarios take place near criticality, one is above (STM-driven) and the other (LTM-driven) just below the critical point. Hence, both are valid but obtained under different criteria as we explain next. In this Section we describe the STM-driven mechanism for ITM, and in the next one the LTM-driven. For the STM-driven, we simulate it in the region (gray area in Fig. 4 a) which includes

only the dormant steady state. However, due to its closeness to the LTM, the forgetting process is slow, and might include a long plateau which acts as a quasi-steady state, for some period. This means that, in the ω -space, ITM has $\omega < \omega_c$ and therefore converges to zero, however, its ω is near criticality and hence it changes slowly in a plateau shape, while passing near the transition (ω_c, I_c) such that it is a pseudo-steady state, see Fig. 4 a - b (see also the analogous plateau phenomena in percolation of interdependent networks [24]). Note that for the ITM (quasi-steady state long plateau) current simulations in Fig. 4 b, we used much smaller values of $\Delta\omega$ (i.e., $\omega \rightarrow \omega_c$), compared to our STM simulations in Fig. 3 b.

The duration of this slow decaying plateau depends on the proximity of ω to ω_c , as depicted next (as in [25], see also similar plateau behavior in interdependent networks [24]). In general, the time between two points with 2ϵ currents difference can be described as:

$$T = \int dt = \int_{I_c+\epsilon}^{I_c-\epsilon} \frac{dt}{dI} dI = \int_{I_c+\epsilon}^{I_c-\epsilon} \left(\frac{dI}{dt} \right)^{-1} dI \approx \tau \int_{-\epsilon}^{\epsilon} \left(-\tau \frac{d\delta I}{dt} \right)^{-1} d\delta I. \quad (14)$$

To calculate the argument of the integral, we analyze the behavior of Eq. (5) in the limit of $\omega \rightarrow \omega_c^- = e \cdot C(N-1)$ and $I \rightarrow I_c = e \cdot C$. This is since in this regime the system decays at a minimal speed and hence spends a maximal time. We further use Eq. (11) for small $\Delta\omega$, but this time we keep also the second order term of δI ,

$$-\tau \frac{d\delta I}{dt} \approx \frac{I_c}{2} \left[\left(\frac{\delta I}{I_c} \right)^2 + 2 \frac{\Delta\omega}{\omega_c} \frac{\delta I}{I_c} + 2 \frac{\Delta\omega}{\omega_c} \right]. \quad (15)$$

Placing Eq. (15) into Eq. (14), yields,

$$T \approx 2\tau \int_{-\infty}^{\infty} \frac{1}{x^2 + 2bx + 2b} dx = \frac{2\tau\pi}{\sqrt{b}\sqrt{2-b}}, \quad (16)$$

where $x = \delta I/I_c$ and $b = \Delta\omega/\omega_c$. Note that in Eq. (16) the integration limits are $\pm\infty$, since at $\omega \rightarrow \omega_c$ the major contribution to the duration of the plateau is when I is close to I_c , hence more accurate borders do not impact the leading term.

Since $b = \Delta\omega/\omega_c$ is small, we finally get the plateau duration,

$$T \approx \tau \frac{\sqrt{2}\pi}{\sqrt{\Delta\omega/\omega_c}}. \quad (17)$$

Figure 4 c illustrates the good fit between the theory, Eq. (17) (red line), and the simulations results (blue dots). As expected, this fit is better at low values of $\Delta\omega$, i.e., when ω is closer to criticality.

Furthermore, a closer look on recent empirical studies performed with EPSP measuring LTP of rats models [7, 26], shows ITM with a quasi-steady state long plateau similar to our theory and simulation results. Fig. 4 d compares between LTP of aged rats [7] (blue dots) to simulating the current with ω close to criticality ($\Delta\omega/\omega_c = 0.04$). The excellent agreement between the plateau simulations and the EPSP measurements, suggests that the average synaptic strength relates to the critical synaptic strength as $\omega = 0.96\omega_c$. We note that similar plateau behavior has been also observed for EPSP measuring LTP of pilocarpine-treated rats [26].

Intermediate-term memory(ITM): LTM-driven

Our results of studying memory loss dynamics suggest that ITM can be initiated as either LTM (ITM-LTM-driven) or STM (ITM-STM-driven), with averaged synaptic strength close to the critical value. While in previous section we focused on the ITM-STM-driven, and relate it to aged rats, here we focus on the ITM-LTM-driven scenario to obtain an ITM, which we relate to young rats. In the previous section ITM has been obtained from STM close to criticality, while here the ITM is obtained from LTM close to criticality. Only this time, the scenario of ITM

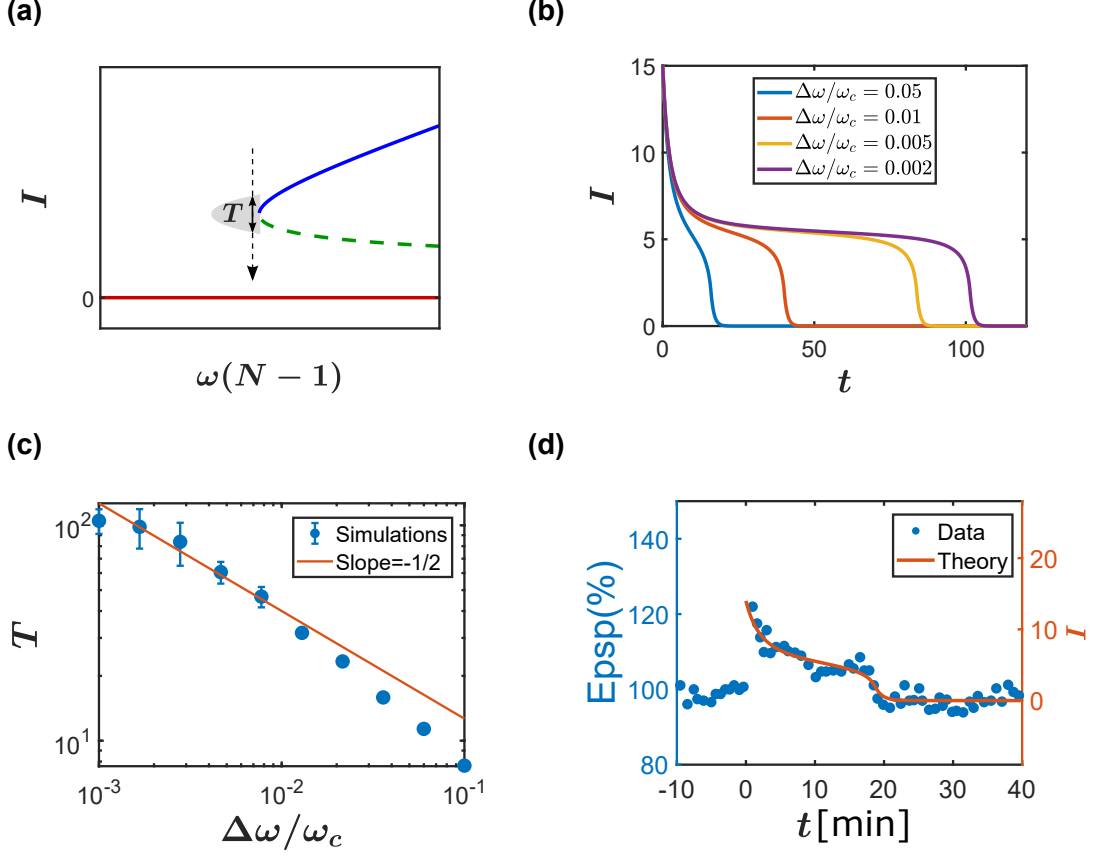


Figure 4: Plateau: ITM-STM-driven. (a) The ITM-STM-driven scenario describes current that appears below the criticality but close to it. Due to the closeness to the fixed point the current decays towards zero very slowly, such that a pseudo LTM emerges. (b) Below criticality, $\omega < \omega_c$, the average current decays to zero, however close to criticality there is a long slow decay which is similar to a steady state. This quasi-steady state plateau changes its length when simulating with changing the values of $\Delta\omega/\omega_c$. (c) The duration of the plateau is scaled as $\Delta\omega^{-1/2}$ such as depicted in Eq. (17). Here we show averaged values of simulations over 10 realizations concerning Gaussian distribution of the synaptic weights. Simulations in panels (b) and (c) were performed with $\tau = 1$, $C = 2$ and $N = 100$. (d) Temporal LTP experimental data of anesthetized aged rats [7] (blue dots), shows a very good agreement with our theoretical simulation results (red line) for our suggested state variable $\Delta\omega/\omega_c = 0.04$ (i.e., $\omega = 0.96\omega_c$). All stimulations use $I_0 = 14$, $\tau = 1$ and $C = 2$.

is derived from noise fluctuations of the external current input I_{Aff} , which at a certain point experiences decay towards the dormant state regime.

We extend the model in Eq. (2) so that I_{Aff} is of normal distribution with std σ , according to the following stochastic differential equation:

$$\tau \frac{dI}{dt} = -I + \omega(N-1) \ln\left(\frac{I}{C}\right) \theta(I-C) + \tau \cdot \sigma \cdot n(t), \quad (18)$$

where $n(t)$ is a white noise. We assume that the stimulating current I_0 , which initiates the LTM, has terminated so that now the input I_{Aff} fluctuates around zero. Note that here we analyze the average case with a current averaged over all neurons, same as in the definition, Eq. (2).

In case of ITM, we ask: when will the average current I , which here evolves randomly, cross down a critical value (the threshold, C , in the average case), and consequently the system will collapse to dormant state regime, i.e., fully forgetfulness state. In fact, this phenomenon actually describes the problem of the ‘first passage time’ of a stochastic process [27]. Specifically, we wish to examine the time when on average the mean current I crosses down the threshold C , and consequently decays to the forgetfulness state. In order for this forgetfulness scenario to occur, ω must have a value slightly above the critical ω_c , so that the noise could push it towards the dormant

state regime. Since this occurrence starts as LTM, we denote this as the ITM-LTM-driven mechanism.

In Fig. 5 a we simulate Eq. (18), i.e., the ITM-LTM-driven, with $\sigma = 0.17$ and $\omega = 1.006 \cdot \omega_c$, that is ω slightly above ω_c . Starting at LTM state close to the critical ω_c , due to the I_{Aff} fluctuations, the current I rapidly drops to zero at around $T \approx 400$ [min], hence the memory state is terminated, similar to ITM. The results of 1000 realizations of simulating Eq. (18), all with $\omega = 1.006 \cdot \omega_c$ but with different values of variance σ^2 , are shown in Fig. 5 b. The average forgetfulness time $\langle T \rangle$, of all realizations, shows an inverse relation to σ^2 , seen by the dashed line.

Our LTP data analysis in Fig. 2 d of young rats shows ω slightly above criticality (also $\omega = 1.006 \cdot \omega_c$), where the memory was reported to vanish eventually after a week [7], much shorter than expected from LTM (lasting many years). Hence this case fits well to our stochastic ITM-LTM-driven definition. According to our findings of the ω values, we suggest that while aged rats could show ITM-STM-driven (slightly below the critical ω_c , with $\omega = 0.96 \cdot \omega_c$, Fig. 4 d), young rats might show ITM-LTM-driven (ω slightly above ω_c , with $\omega = 1.006 \cdot \omega_c$ Fig. 2 d).

Theoretically, we can use Fig. 5 b simulation results to evaluate the neuronal noise σ . Terminating the LTP memory data in Fig. 2 d after around one week [7], i.e., $\langle T \rangle \approx 10,000$ [min], according to Fig. 5 b it fits to a value of $\sigma^2 \approx 10^{-2}$, hence $\sigma \approx 0.1$. The units of σ are determined by the appropriate current excitability threshold C . For example, if $C = 80 pA$ [28] for the rat current excitability threshold, then the units are $80/2 pA$ (i.e., divided by our threshold $C = 2$), hence the average neuronal noise is $\sigma = 0.1 \cdot 80/2 = 4 pA$. This value of σ is in agreement with the estimated value of $4.4 pA$ current noise of single neuron, as was suggested when investigating cultured neurons from rat hippocampus held near activation potential [29].

In conclusion, we present here and in the previous section, two possible scenarios for ITM: (i) derived from STM close to criticality (just below) creating a plateau (Fig. 4), or (ii) derived from LTM close to criticality (just above) with fluctuations that at a point drops below criticality (Fig. 5 a). Both options yield similar current trajectory, however, originate from different mechanisms. While the ITM-LTM-driven at Fig. 5 starts its course as LTM and is terminated due to stochasticity nature, in the ITM-STM-driven in Fig. 4 the current starts at the STM close to criticality and therefore is terminated from stabilizations considerations.

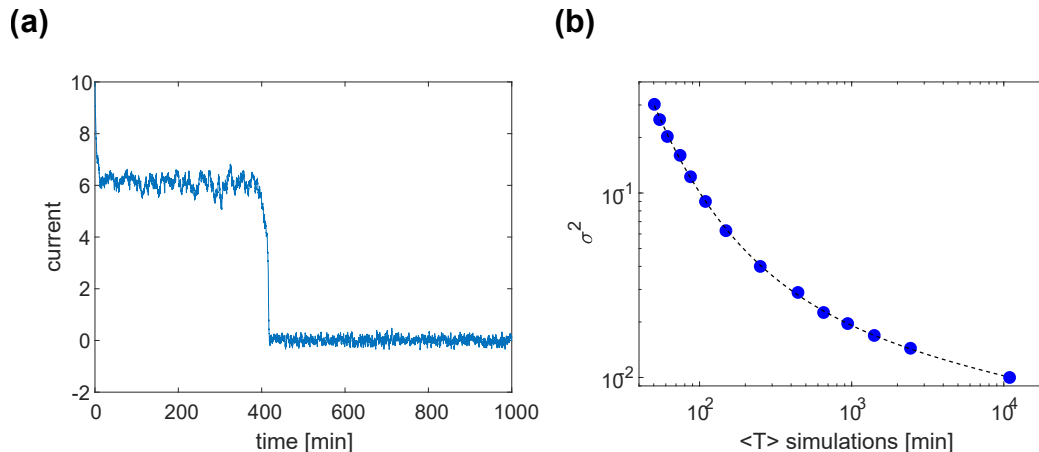


Figure 5: Simulations of neuronal noise: ITM-LTM-driven with white noise. (a) In the LTM phase when close to criticality, there is a chance that afferent input noise will lead to crossing the criticality towards the forgetting region. The average current evolves in time according to Eq. (18). Simulating the case $\Delta\omega/\omega_c = 0.006$ and $\sigma = 0.17$, yields a first passage time T , where the current I sharply decays below the threshold C , at around $T \approx 400$ [min]. (b) The average time until forgetting $\langle T \rangle$, calculated as the averaged duration time from 1,000 simulations realizations, is marked in blue dots. As σ decreases, the mean time duration $\langle T \rangle$ increases inversely, dashed line. All simulations here were performed with $\tau = 1$ [min] [30] and $N = 100$. The units of $\langle T \rangle$ are in [min], same as the units of τ .

Discussion

In the present work we analytically describe fundamental dynamics of STM, LTM and ITM, by exploring the effects of the strength of the neuronal network synaptic connections on memory decay in time. Generally, our theory explains the conventional empirical description of memory decay as exponential with two characteristic times [2, 3]. We find that the second exponent towards the end of the memory signal is mainly important for its direct relation to the average synaptic strength. Specifically, the temporal description of the region above the steady state memory defines three time constants: τ_{LT} for LTM, τ_{ST} for STM, and T or $\langle T \rangle$ for ITM, for which we provide analytical relations to the average synaptic strength (Eq. (10), Eq. (13) and Eq. (17)). Interestingly, all three time constants depend on ω_c and τ , which might explain the empirical findings of correlations [22, 23] between all memory types.

For our working memory model analysis, we used the neuronal network connections effects on the membrane currents through a logarithmic function (Eq. (1)) in accordance with previous studies on memory [9, 5]. While other functions can be used, for example hyperbolic tangent [31] or with a delay [32], we expect similar conclusions without changing the main inferences, though the ω -space diagram in Fig. 1, might be quantitatively changed for the different functions [33].

Our analytical approach to memory has two sides, on one hand we provide a clear distinction between STM and LTM as above and below a critical value (ω_c), and on the other hand we provide spectrum of descriptions for ITM. Specifically, for the ITM we offer two scenarios that originate from being close to criticality, one begins at STM and the other begins at LTM. We assume that both scenarios are relevant and apply to different possible cases.

Exploring empirical studies of animal models, we manage, based on our framework, to evaluate the ω/ω_c state variable, which represents the normalized average synaptic strength. In particular, for the LTP empirical work performed on anesthetized rats model: young vs. aged [7], we find only a small difference of $\omega/\omega_c = 1.006$ vs. $\omega/\omega_c = 0.96$ (respectively) when analyzing Fig. 2 d vs. Fig. 4 d. The finding for the young rats $\omega/\omega_c = 1.006$ LTM close to criticality (i.e., close to 1) suggests that it is not surprising that for the same experimental protocol aged rats show ω/ω_c just below criticality. The reasons for the LTP protocols to reach only close to criticality, and not much beyond, could be diverse. For example, it could happen since the rats are anesthetized and therefore cannot produce higher ω . Another reason could be attributed to the LTP protocol itself, perhaps more extended stimulation is needed to reach larger ω . Nevertheless, here we offer that LTP does not evolve to LTM since it produces synaptic strength which is too weak, with value just above or just below criticality for young and aged anesthetized rats respectively. We note that additional work is required to further distinguish between our two suggested ITM mechanisms, namely between ITM-LTM-driven and ITM-STM-driven, for example exploring possible difference of the current probability distributions.

Equation (17) and Fig. 5 describe analytically and via simulations respectively the typical time duration of the ITM-STM-driven and the ITM-LTM-driven cases respectively. While for the ITM-STM-driven case we offer deterministic approach, for the ITM-LTM-driven case we offer a stochastic mechanism. From Fig. 5 we conclude that as the noise level σ increases, the memory terminates earlier and there is a higher probability to return to stable dormant state (no-memory state). However, the opposite scenario, i.e., obtaining memory from the no memory state due to synaptic weight noise, is not possible according to our simulations. Adding synaptic noise to the model during the stable dormant state could not change the state, i.e., did not produce memory, even in proximity to the ω_c critical value. This points on a possible protection mechanism that prevents maintaining false memory, due to merely noise, at the long term (see also supplementary Fig. S2).

The neuronal noise is of clinical importance, that spans diverse clinical implications [30, 34]. Here, our simulations shown in Fig. 5 suggest that medications that reduce neuronal noise level can prolong memory, and hence might even prevent fall risk in dementia patients[35]. On the other spectrum of memory malfunctions, are diseases that are characterized by excessive memory, such as in post-traumatic stress disorder (PTSD). In those situations the patients might benefit from medications that promote forgetfulness by increasing synaptic noise. Generally,

forgetfulness is an important mechanism, allowing acquisition of new memories, our suggested ITM-LTM-driven could serve as an integral part of a healthy forgetfulness mechanism.

References

- [1] H. Ebbinghaus, Memory (ha ruger & ce bussenius, trans.). *New York: Teachers College.(Original work published 1885)* **39** (1913).
- [2] D. C. Rubin, S. Hinton, A. Wenzel, The precise time course of retention. *Journal of Experimental Psychology: Learning, Memory, and Cognition* **25**, 1161 (1999).
- [3] M. A. Erickson, L. A. Maramara, J. Lisman, A single brief burst induces glur1-dependent associative short-term potentiation: a potential mechanism for short-term memory. *Journal of cognitive neuroscience* **22**, 2530–2540 (2010).
- [4] M. A. Sutton, S. E. Masters, M. W. Bagnall, T. J. Carew, Molecular mechanisms underlying a unique intermediate phase of memory in aplysia. *Neuron* **31**, 143–154 (2001).
- [5] D. Durstewitz, J. K. Seamans, T. J. Sejnowski, Neurocomputational models of working memory. *Nature neuroscience* **3**, 1184–1191 (2000).
- [6] G. Mongillo, O. Barak, M. Tsodyks, Synaptic theory of working memory. *Science* **319**, 1543–1546 (2008).
- [7] M. A. Lynch, Long-term potentiation and memory. *Physiological reviews* **84**, 87–136 (2004).
- [8] D. Hebb, Organization of behavior. new york: Wiley. *J. Clin. Psychol* **6**, 335–307 (1949).
- [9] D. J. Amit, N. Brunel, Learning internal representations in an attractor neural network with analogue neurons. *Network: Computation in Neural Systems* **6**, 359–388 (1995).
- [10] J. E. Lisman, J.-M. Fellous, X.-J. Wang, A role for nmda-receptor channels in working memory. *Nature neuroscience* **1**, 273–275 (1998).
- [11] F. Barbieri, N. Brunel, Can attractor network models account for the statistics of firing during persistent activity in prefrontal cortex? *Frontiers in neuroscience* **2**, 114–122 (2008).
- [12] D. J. Amit, N. Brunel, Model of global spontaneous activity and local structured activity during delay periods in the cerebral cortex. *Cerebral cortex (New York, NY: 1991)* **7**, 237–252 (1997).
- [13] N. Cowan, What are the differences between long-term, short-term, and working memory? *Progress in brain research* **169**, 323–338 (2008).
- [14] J. J. Hopfield, Neural networks and physical systems with emergent collective computational abilities. *Proceedings of the national academy of sciences* **79**, 2554–2558 (1982).
- [15] J. J. Hopfield, Neurons with graded response have collective computational properties like those of two-state neurons. *Proceedings of the national academy of sciences* **81**, 3088–3092 (1984).
- [16] J. Gao, B. Barzel, A.-L. Barabási, Universal resilience patterns in complex networks. *Nature* **530**, 307–312 (2016).
- [17] S. Solomon, B. Shir, Complexity; a science at 30. *Europhysics news* **34**, 54–57 (2003).
- [18] E. Ben-Naim, H. Frauenfelder, Z. Toroczkai, *Complex networks*, vol. 650 (Springer Science & Business Media, 2004).

- [19] M. Gosak, R. Markovič, J. Dolensek, M. S. Rupnik, M. Marhl, A. Stožer, M. Perc, Network science of biological systems at different scales: A review. *Physics of life reviews* **24**, 118–135 (2018).
- [20] R. L. Stoop, N. Stoop, K. Kanders, R. Stoop, Excess entropies suggest the physiology of neurons to be primed for higher-level computation. *Physical Review Letters* **127**, 148101 (2021).
- [21] W. A. Wickelgren, Time, interference, and rate of presentation in short-term recognition memory for items. *Journal of Mathematical Psychology* **7**, 219–235 (1970).
- [22] N. Unsworth, On the division of working memory and long-term memory and their relation to intelligence: A latent variable approach. *Acta psychologica* **134**, 16–28 (2010).
- [23] C. A. Was, D. J. Woltz, Reexamining the relationship between working memory and comprehension: The role of available long-term memory. *Journal of Memory and Language* **56**, 86–102 (2007).
- [24] D. Zhou, A. Bashan, R. Cohen, Y. Berezin, N. Shnerb, S. Havlin, Simultaneous first-and second-order percolation transitions in interdependent networks. *Physical Review E* **90**, 012803 (2014).
- [25] S. H. Strogatz, *Nonlinear dynamics and chaos: with applications to physics, biology, chemistry, and engineering* (CRC press, 2018).
- [26] S. Grosser, N. Buck, K.-H. Braunewell, K. E. Gilling, C. Wozny, P. Fidzinski, J. Behr, Loss of long-term potentiation at hippocampal output synapses in experimental temporal lobe epilepsy. *Frontiers in Molecular Neuroscience* p. 143 (2020).
- [27] S. Redner, *A guide to first-passage processes* (Cambridge university press, 2001).
- [28] T. Tateno, A. Harsch, H. Robinson, Threshold firing frequency–current relationships of neurons in rat somatosensory cortex: type 1 and type 2 dynamics. *Journal of neurophysiology* **92**, 2283–2294 (2004).
- [29] K. Diba, H. A. Lester, C. Koch, Intrinsic noise in cultured hippocampal neurons: experiment and modeling. *Journal of Neuroscience* **24**, 9723–9733 (2004).
- [30] H. Dvir, I. Elbaz, S. Havlin, L. Appelbaum, P. C. Ivanov, R. P. Bartsch, Neuronal noise as an origin of sleep arousals and its role in sudden infant death syndrome. *Science advances* **4**, eaar6277 (2018).
- [31] A. Lansner, Associative memory models: from the cell-assembly theory to biophysically detailed cortex simulations. *Trends in neurosciences* **32**, 178–186 (2009).
- [32] S. Leng, W. Lin, J. Kurths, Basin stability in delayed dynamics. *Scientific reports* **6**, 1–6 (2016).
- [33] H. Sanhedrai, J. Gao, A. Bashan, M. Schwartz, S. Havlin, B. Barzel, Reviving a failed network through microscopic interventions. *Nature Physics* pp. 1–12 (2022).
- [34] H. Dvir, J. W. Kantelhardt, M. Zinkhan, F. Pillmann, A. Szentkiralyi, A. Obst, W. Ahrens, R. P. Bartsch, A biased diffusion approach to sleep dynamics reveals neuronal characteristics. *Biophysical journal* **117**, 987–997 (2019).
- [35] P. L. Sheridan, J. M. Hausdorff, The role of higher-level cognitive function in gait: executive dysfunction contributes to fall risk in alzheimer’s disease. *Dementia and geriatric cognitive disorders* **24**, 125–137 (2007).

Supplementary information

S.1 Mean-field approximation

Starting with Eq. (1) in the main text,

$$\tau \frac{dI_i}{dt} = -I_i + \sum_{j \neq i} w_{ij} \ln \left(\frac{I_j}{C} \right) \theta(I_j - C) + I_{\text{Aff}}, \quad (\text{S.1})$$

we use a mean-field approach and assume that since the summation is on large number of variables from a narrow distribution due to their similar degrees and weight distribution, we can replace the variables I_j by their average over the entire network, I , yielding

$$\tau \frac{dI_i}{dt} = -I_i + \sum_{j \neq i} w_{ij} \ln \left(\frac{I}{C} \right) \theta(I - C) + I_{\text{Aff}}, \quad (\text{S.2})$$

where the average current is simply

$$I = \frac{1}{N} \sum_{i=1}^N I_i. \quad (\text{S.3})$$

Next, we operate an averaging on Eq. (S.2),

$$\frac{1}{N} \sum_{i=1}^N \tau \frac{dI_i}{dt} = \frac{1}{N} \sum_{i=1}^N (-I_i) + \frac{1}{N} \sum_{i=1}^N \sum_{j \neq i} w_{ij} \ln \left(\frac{I}{C} \right) \theta(I - C) + I_{\text{Aff}}, \quad (\text{S.4})$$

by which we obtain Eq. (2) in the main text,

$$\tau \frac{dI}{dt} = -I + \omega(N-1) \ln \left(\frac{I}{C} \right) \theta(I - C) + I_{\text{Aff}}, \quad (\text{S.5})$$

where

$$\omega = \frac{1}{N(N-1)} \sum_{i=1}^N \sum_{j \neq i} w_{ij} \quad (\text{S.6})$$

is the average weight.

S.2 Fixed points and stability analysis

To find the fixed points of the system including both stable and unstable states, we just demand relaxation in Eq. (5) in the main text, i.e. $dI/dt = 0$,

$$0 = -I + \omega(N-1) \ln \left(\frac{I}{C} \right) \theta(I - C), \quad (\text{S.7})$$

whose solutions are the fixed points.

To classify whether a solution of Eq. (S.7) is stable, we demand the known stability condition [25],

$$\frac{\partial}{\partial I} \left(\frac{dI}{dt} \right) < 0. \quad (\text{S.8})$$

One can see that the fixed point $I = 0$ is stable since the term in Eq. (S.8) is $-1 < 0$. There are also positive stable fixed points, see Fig. S1. In between, there exist unstable fixed points (dashed line) separating between the basins of attraction of the stable states.

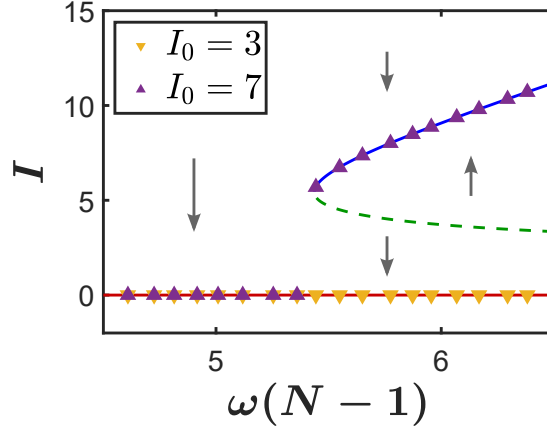


Figure S1: Memory phase diagram. The phase diagram in ω -space yielded by Eqs. (S.5),(S.7),(S.8). The blue and the red continuous lines represent the steady states, while the dashed green line represents an unstable state separating between the two basins of attraction. Simulation (symbols) with normally distributed synaptic weights with $\sigma = \omega_c/4$ starting with high (purple) and low (orange) initial conditions are shown for $N = 100$, $\tau = 1$ and $C = 2$.

S.3 Tipping point

To find the critical (tipping) point (ω_c, I_c) of the transition from STM to LTM, shown in Fig. S1, we notice that this point is a junction of a stable fixed point (continuous blue line in Fig. S1) and unstable one (dashed green line), resulting in vanishing of the term in Eq. (S.8). Therefore, two conditions should be satisfied in the critical point:

1. fixed point, 2. a transition from unstable to stable, as follows,

$$\begin{aligned} 1. \quad & \frac{dI}{dt} = 0, \\ 2. \quad & \frac{\partial}{\partial I} \left(\frac{dI}{dt} \right) = 0. \end{aligned} \quad (\text{S.9})$$

Using Eq. (5) in the main text, we obtain,

$$\begin{aligned} 1. \quad & -I_c + \omega_c(N-1) \ln \left(\frac{I_c}{C} \right) = 0, \\ 2. \quad & -1 + \omega_c(N-1) \frac{1}{I_c} = 0. \end{aligned} \quad (\text{S.10})$$

The solution is

$$\omega_c = \frac{e \cdot C}{N-1}, \quad (\text{S.11})$$

and

$$I_c = \omega_c(N - 1) = e \cdot C, \quad (\text{S.12})$$

as given in Eq. 6 in the main text.

S.4 LTM typical relaxation time

To get the current exponential decay for $\omega > \omega_c$, in the limit of $I \rightarrow I_{\text{LT}}$, we expand Eq. (5) in the main text as $I = I_{\text{LT}} + \delta I$ where δI is small, and obtain,

$$\tau \frac{d\delta I}{dt} = -I_{\text{LT}} - \delta I + \omega(N - 1) \ln \left(\frac{I_{\text{LT}} + \delta I}{C} \right), \quad (\text{S.13})$$

which can be written as

$$\tau \frac{d\delta I}{dt} = -I_{\text{LT}} - \delta I + \omega(N - 1) \left[\ln \left(\frac{I_{\text{LT}}}{C} \right) + \ln \left(1 + \frac{\delta I}{I_{\text{LT}}} \right) \right]. \quad (\text{S.14})$$

Using Eq. (7) in the main text, and expanding $\ln(1 + \epsilon)$ for small δI (Taylor series), we obtain

$$\tau \frac{d\delta I}{dt} \approx - \left(1 - \frac{\omega(N - 1)}{I_{\text{LT}}} \right) \delta I - \frac{1}{2} \omega(N - 1) \left(\frac{\delta I}{I_{\text{LT}}} \right)^2. \quad (\text{S.15})$$

Neglecting the second order term (which is equivalent to assuming $\delta I/I_{\text{LT}} \ll \ln(I_{\text{LT}}/I_c)$), and additionally using Eq. (7) again, we obtain

$$\tau \frac{d\delta I}{dt} \approx - \left(1 - \frac{1}{\ln(I_{\text{LT}}/C)} \right) \delta I. \quad (\text{S.16})$$

This implies an exponential decay with typical time decay

$$\tau_{\text{LT}} = \frac{\tau}{1 - \frac{1}{\ln(I_{\text{LT}}/C)}}, \quad (\text{S.17})$$

which is Eq. (9) in the main text.

S.4.1 Close to criticality

Next, we evaluate τ_{LT} when ω is close to the critical value ω_c from above. To track the behavior in proximity to ω_c (for small $\Delta\omega$), we expand Eq. (7) by $\omega = \omega_c + \Delta\omega$ and $I_{\text{LT}} = I_c + \delta I_{\text{LT}}$. Recalling $I_c = e \cdot C$, $\omega_c = e \cdot C / (N - 1)$ (Eq. (6)), we get

$$0 = -e \cdot C - \delta I_{\text{LT}} + (e \cdot C + \Delta\omega(N - 1)) \ln(e + \delta I_{\text{LT}}/C), \quad (\text{S.18})$$

which is

$$0 = -I_c - \delta I_{\text{LT}} + (I_c + \Delta\omega(N - 1)) \left[1 + \ln \left(1 + \frac{\delta I_{\text{LT}}}{I_c} \right) \right]. \quad (\text{S.19})$$

Expansion of $\ln(1 + \epsilon)$ for small ϵ gives

$$0 \approx -I_c - \delta I_{\text{LT}} + (I_c + \Delta\omega(N - 1)) \left[1 + \frac{\delta I_{\text{LT}}}{I_c} - \frac{\delta I_{\text{LT}}^2}{2I_c^2} + \dots \right]. \quad (\text{S.20})$$

This yields

$$\delta I_{\text{LT}} \approx I_c \sqrt{2\Delta\omega/\omega_c}. \quad (\text{S.21})$$

Substituting this into Eq. (9), we finally get

$$\tau_{\text{LT}} = \frac{\tau}{1 - \frac{1}{\ln(e + \delta I_{\text{LT}}/C)}} \approx \frac{\tau}{1 - \frac{1}{1 + \delta I_{\text{LT}}/(e \cdot C)}} \approx \frac{\tau}{\delta I_{\text{LT}}/I_c}. \quad (\text{S.22})$$

Hence, close to criticality, $\omega \rightarrow \omega_c$ (though still $\omega > \omega_c$),

$$\tau_{\text{LT}} \approx \frac{\tau}{\sqrt{2\Delta\omega/\omega_c}}, \quad (\text{S.23})$$

which is Eq. (10) in the main text.

S.5 STM typical time decay

For exploring the exponential decay in $\omega < \omega_c$ region, we analyze the evolution of $I(t)$ around I_c . Therefore, we define here $\omega = \omega_c - \Delta\omega$ (this is in contrast to the LTM where $\omega > \omega_c$ which defines $\omega = \omega_c + \Delta\omega$). Let us expand Eq. (5) in the main text at $I = I_c + \delta I$, for small deviation δI ,

$$\tau \frac{dI}{dt} = -I + (\omega_c - \Delta\omega)(N - 1) \ln \left(\frac{I_c + \delta I}{C} \right), \quad (\text{S.24})$$

that is,

$$\tau \frac{dI}{dt} = -I + (\omega_c - \Delta\omega)(N - 1) \left[\ln \left(\frac{I_c}{C} \right) + \ln \left(1 + \frac{\delta I}{I_c} \right) \right]. \quad (\text{S.25})$$

Recalling $I_c = e \cdot C$ and $\omega_c = e \cdot C/(N - 1)$, Eq. (6), and expanding the Taylor series of $\ln(1 + \epsilon)$ to the first order, we get

$$\tau \frac{dI}{dt} \approx -I + (I_c - \Delta\omega(N - 1)) \left[1 + \frac{\delta I}{I_c} - \frac{1}{2} \left(\frac{\delta I}{I_c} \right)^2 \right] \approx -\frac{\Delta\omega}{\omega_c} I, \quad (\text{S.26})$$

where we neglect the second order term, *i.e.* we assume $(\delta I/I_c)^2 \omega(N - 1) \ll (I_c + \delta I)\Delta\omega/\omega_c$. Thus, this region gets smaller close to criticality ω_c , as illustrated in Fig. 3 a in the main text (this region is marked in gray).

Finally, Eq. (S.26) yields

$$I(t) \sim \exp(-t/\tau_{\text{ST}}), \quad (\text{S.27})$$

where the time decay is

$$\tau_{\text{ST}} = \frac{\tau}{\Delta\omega/\omega_c}, \quad (\text{S.28})$$

which is Eq. (13) in the main text.

S.6 Memory creation

Figure S2 demonstrates, based on Eq. (2) in the main text, the possibility of creation memory. The memory is generated due to the contemporary existence of $I_{\text{Aff}} > C$ which causes to the increasing of I . Once the stimulation finished and I_{Aff} vanished, the current decays either to its long-term memory steady state or to zero in the case of short-term memory as shown in Fig. 1. One can see in Fig. S2a that for large weight, $\omega > \omega_c$, and $I_{\text{Aff}} > C$, *i.e.* right to the point at which the curve gets broken, a long-term memory is created (light blue arrow). This is because the current increases much during the stimulation, and once I_{Aff} becomes zero, the current decreases to the high stable state (blue), and stays there. In contrast, if $I_{\text{Aff}} < C$ (orange arrow), the current increases slightly to the low stable state (red), such as when $I_{\text{Aff}} = 0$, the current decays to zero, and no memory has been created. While for $\omega < \omega_c$, as shown in Fig. S2b, even if the stimulation is strong (light blue arrow), no long-term memory is created since, there is no high stable state for $I_{\text{Aff}} = 0$, thus the current decays to zero.

However, note that the right tipping point (intersection of red and green lines) does not change with ω . Thus, the condition of a major stimulation is always $I_{\text{Aff}} > C$ independent on ω . The weight ω impacts only the ability of the system to preserve the memory for a long term. Therefore, a noise in the weights cannot cause an emergence of a memory although it can cause a loss of a memory as shown in Fig. 5.

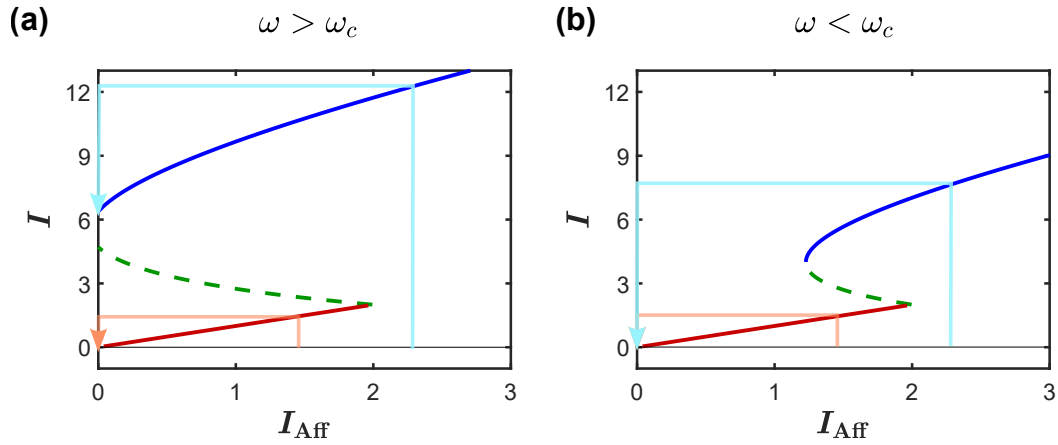


Figure S2: Creation of memory. While noise in the weights greatly affect memory loss (change the state from memory state $\omega > \omega_c$ to no memory state - see Fig. 5), the appearance of noise in the no memory state ($\omega < \omega_c$) cannot change the state toward memory. This effect can be understood from the illustration of the states with (a) $\omega > \omega_c$ and (b) $\omega < \omega_c$. Whereas changing ω greatly affects the stable memory state (in blue) and the left transition point, the stable no-memory state (in red) and the right transition point remain unaffected. Hence, variations in ω cannot affect the no-memory stable state.